Seasonality and the Coexistence of Pathogen Strains

Viggo Andreasen[1] and Greg Dwyer[2,*]

1. Mathematics and Physics (IMFUFA), Department of Science, Roskilde University, Roskilde, Denmark; 2. Department of Ecology and Evolution, University of Chicago, Chicago, Illinois 60637

Submitted February 19, 2020; Accepted September 29, 2022; Electronically published March 30, 2023

Online enhancements: supplemental PDF.

ABSTRACT: Host-pathogen models usually explain the coexistence of pathogen strains by invoking population structure, meaning host or pathogen variation across space or individuals; most models, however, neglect the seasonal variation typical of host-pathogen interactions in nature. To determine the extent to which seasonality can drive pathogen coexistence, we constructed a model in which seasonal host reproduction fuels annual epidemics, which are in turn followed by interepidemic periods with no transmission, a pattern seen in many host-pathogen interactions in nature. In our model, a pathogen strain with low infectiousness and high interepidemic survival can coexist with a strain with high infectiousness and low interepidemic survival: seasonality thus permits coexistence. This seemingly simple type of coexistence can be achieved through two very different pathogen strategies, but understanding these strategies requires novel mathematical analyses. Standard analyses show that coexistence can occur if the competing strains differ in terms of R_0, the number of new infections per infectious life span in a completely susceptible population. A novel mathematical method of analyzing transient dynamics, however, allows us to show that coexistence can also occur if one strain has a lower R_0 than its competitor but a higher initial fitness λ_0, the number of new infections per unit time in a completely susceptible population. This second strategy allows coexisting pathogens to have quite similar phenotypes, whereas coexistence that depends on differences in R_0 values requires that coexisting pathogens have very different phenotypes. Our novel analytic method suggests that transient dynamics are an overlooked force in host-pathogen interactions.

Keywords: heritability, trade-offs, host-pathogen system, complex dynamics, eco-evolutionary.

Introduction

Mathematical theories of pathogen competition have achieved important successes in understanding pathogen virulence, notably by showing that trade-offs between pathogen fitness components can lead to natural selection for intermediate virulence (Anderson and May 1982). Observations of trade-offs and virulence evolution have provided empirical support for trade-off theory (Alizon et al. 2009; Leggett et al. 2013; Alizon and Michalakis 2015), but simple trade-off models cannot explain the coexistence of competing pathogen strains (Keeling and Rohani 2008). Pathogen coexistence has nevertheless been widely observed in the field (Hellard et al. 2015; Betts et al. 2016; Fountain-Jones et al. 2018), confirming that simple trade-off theory is not sufficient to describe pathogen coexistence in nature.

More complex models have explained pathogen coexistence using a range of mechanisms, including pathogen specialization on particular host genotypes (Lively and Dybdahl 2000), spatial aggregation of pathogen strains (Messinger and Ostling 2009), host density-dependent mortality (Andreasen and Pugliese 1995), and a balance between within-host and between-host competitive ability (Levin and Pimentel 1981; Clay et al. 2019). A common feature of these disparate models is variation in host or pathogen densities across space or individuals and thus population structure broadly defined (Briggs et al. 2010; Lion et al. 2011). The theoretical literature therefore suggests a loose consensus that pathogen coexistence is best explained by population structure in the host, the pathogen, or both.

Here, we propose that pathogen coexistence may alternatively be explained by variation across time, in the form of seasonality in host reproduction and pathogen transmission. Standard host-pathogen models assume that host reproduction and pathogen transmission are nonseasonal, an assumption that reflects the origin of the models as models of infectious diseases of humans (Keeling and Rohani 2008). In infectious diseases of animals and plants, in contrast, seasonality in host reproduction and pathogen transmission is the rule rather than the exception (Altizer et al. 2006; van den Berg et al. 2010; Filion et al. 2020; Poulin 2020).

Recognition of the ubiquity of seasonality has led to the increasing use of seasonal models in disease ecology (Altizer et al. 2006; Mordecai et al. 2016). Models of the

* Corresponding author; email: gdwyer@uchicago.edu.
ORCIDs: Dwyer, https://orchid.org/0000-0002-7387-2075.

  https://doi.org/10.1086/723490

effects of seasonality on pathogen coexistence, however, have to our knowledge considered only the particular case in which coexistence can result from evolutionary branching, in which a single pathogen strain gives rise to two strains through a series of small phenotypic changes (van den Berg et al. 2010; Hamelin et al. 2011). This approach usefully describes how mutational dynamics can lead to coexistence, but it cannot easily be used to understand the ecological mechanisms by which seasonality allows for pathogen coexistence and thus cannot easily explain how and why pathogens coexist in seasonal environments.

Here, we therefore instead consider pathogen coexistence from an ecological perspective. We construct a model of pathogen competition in a seasonal environment, and we analyze the model to understand the conditions under which seasonality leads to the coexistence of pathogen strains. Using a novel mathematical tool, we derive simple criteria that quantify the range of pathogen phenotypes over which pathogen coexistence can occur. Because coexistence is much more likely if a low-infectiousness/high-survival pathogen strain can cause a high number of infections in the early stages of an epidemic, our work shows that the transient dynamics of epidemics play a key role in pathogen coexistence in seasonal environments. Because our model's structure provides a good approximation to the ecology of pathogens of taxonomically diverse host species, including pathogens of plants, invertebrates, and vertebrates, our research illustrates a general approach to understanding the role of seasonality in pathogen coexistence. We conclude that seasonality provides an important alternative to population structure as an explanation for pathogen coexistence.

Model Construction

Overview

Models of seasonality in host-pathogen interactions have historically followed an approach from human epidemiology in which host reproduction or pathogen transmission is assumed to vary sinusoidally (Altizer et al. 2006; Buonomo et al. 2018). In nature, in contrast, animal and plant reproduction and pathogen transmission usually occur during separate periods, such that a flush of susceptible hosts due to host reproduction leads to an annual pathogen epidemic, which is in turn followed by a long period during which neither host reproduction nor pathogen transmission occurs.

This pattern is most obvious in insect pathogens, in which host reproductive periods are often short (Hunter 1995) and host larvae are often the only susceptible stage (Cory and Myers 2003), and in plant pathogens, in which infection can often occur only in the aboveground tissue that is produced near the beginning of the growing season (van den Berg et al. 2010; Penczykowski et al. 2015; Suffert et al. 2015; Honjo et al. 2020). In vertebrates, in contrast, there is usually no intrinsically immune age class, but vertebrate hosts often either die or become immune during the annual epidemic, and the next epidemic does not begin until new susceptible hosts are produced during the breeding season. This pattern qualitatively matches the seasonal pattern seen in insects and plants and has been observed in fish (Prati et al. 2020), frogs (Valencia-Aguilar et al. 2016; Mihaljevic et al. 2018; McDevitt-Galles et al. 2020), birds (Hosseini et al. 2004; Van Dijk et al. 2014; Lisovski et al. 2017; Martens et al. 2020), small mammals (Begon et al. 2009; Pathak et al. 2011; Langwig et al. 2015), large mammals (Havarua et al. 2014; Beaunée et al. 2015; Treanor et al. 2015; Albery et al. 2018; Scherer et al. 2019), and even sub-Saharan human populations afflicted by measles (Dorélien et al. 2013).

In our model, we therefore assume that there is an annual pathogen epidemic that is fueled by new susceptible hosts produced during a discrete bout of host reproduction. The pathogen is then able to survive the interepidemic period because hosts infected in one epidemic can infect at least a few hosts at the beginning of the following epidemic. Pathogen survival across the interepidemic period may be due either to the persistence of infectious particles in the environment, as occurs in insect pathogens (Murray and Elkinton 1989; Hajek 1999), plant pathogens (Penczykowski et al. 2015), and vertebrate pathogens like avian flu (Rohani et al. 2009), or to asymptomatic hosts that act as carriers that infect susceptible young after the breeding period, as occurs in many different vertebrate pathogens (Becker et al. 2020).

To describe the annual epidemic, we use a SIR-type model from human disease epidemiology (Keeling and Rohani 2008). Following a structure pioneered by Gillespie (1975) and May (1985), we allow for seasonality by embedding the SIR model in a set of difference equations that allow host reproduction to occur in the period between epidemics when the pathogen must survive in the absence of transmission. In previous work with colleagues, we argued that population structure can play a key role in pathogen coexistence in seasonal environments (Fleming-Davies et al. 2015); to focus on the role of seasonality alone, however, here we assume that there are no effects of population structure. To similarly avoid the complication of fluctuating population sizes, we assume that the density of the host is determined by factors other than the pathogen, so that the host population density is the same at the beginning of each epidemic. The same models that we previously used to show that population structure can allow for pathogen coexistence in seasonal environments also suggested that fluctuating population densities make coexistence more likely (Fleming-Davies et al. 2015), suggesting in

turn that our results hold as well for the case of fluctuating population sizes.

Model Equations

Epidemic Submodel. Our SIR-type model tracks the fraction of hosts that are susceptible S, the fraction of hosts that are infected I, and the fraction of hosts that are dead or recovered and immune R; to allow for competition between pathogen strains, we further divide the infected class into hosts infected with a resident strain I_r and hosts infected with an invader strain I_i. For purposes of comparison, we begin with a version of this model that neglects seasonality (Anderson and May 1982):

$$\frac{dS}{dt} = a(S + I_r + I_i + R) - \beta_r SI_r - \beta_i SI_i - \delta S, \quad (1)$$

$$\frac{dI_r}{dt} = \beta_r SI_r - \mu_r I_r - \delta I_r, \quad (2)$$

$$\frac{dI_i}{dt} = \beta_i SI_i - \mu_i I_i - \delta I_i, \quad (3)$$

$$\frac{dR}{dt} = \mu_r I_r + \mu_i I_i - \delta R. \quad (4)$$

Here, a is the host reproductive rate; δ is the nondisease death rate; β_r and β_i are the instantaneous transmission rates of the resident and invader strains of the pathogen, respectively; and μ_r and μ_i are the removal rates of the resident and the invader. Immune hosts cannot be infected by either pathogen strain, but again R can stand for either dead or immune hosts. This model was originally used to describe host-pathogen interactions with fluctuating population sizes (Andreasen and Pugliese 1995); because here we instead assume constant population sizes, in practice we assume $a \equiv \delta$.

For this model, a key quantity is the reproductive number $R_{0,k} = \beta_k/\mu_k$, the number of new infections per old infection in a completely susceptible population, where $k = r$ for the resident and $k = i$ for the invader (throughout, we use k to indicate cases that apply to both the invader and the resident). Because $R_{0,k}$ is the reproductive number when the fraction susceptible $S(t) = 1$ and because $1/\mu_k$ is the average lifetime of an infection, $R_{0,k}$ represents the number of new infections over the pathogen's infectious period and is thus the net number of new infections per infectious life span.

To explain the importance of $R_{0,k}$, we note that if we set $I_i(t) = 0$, then by setting equation (2) to zero we can show that the equilibrium fraction susceptible is $S^* = \mu_r/\beta_r = 1/R_{0,r}$. At this resident-only equilibrium, invasion can occur if $dI_i/dt > 0$, so invasion is possible if $S^* > 1/R_{0,i}$. Substituting $S^* = 1/R_{0,r}$ and rearranging gives a criterion that determines when invasion can occur: $R_{0,i} > R_{0,r}$. In this classical theory, an invasion can thus occur if the invader can maintain the susceptible host population at a lower equilibrium value than the resident; in seasonal environments, in contrast, whether an invasion can occur depends not just on the equilibrium value of the resident but also on the transient dynamics of the invader during epidemics, as we will show.

If $R_{0,i} > R_{0,r}$, then the invader in equations (1)–(4) will drive the resident extinct (Bremermann and Thieme 1989), implying that the strain with the largest $R_{0,k}$ will competitively exclude all other strains. To avoid the unrealistic situation in which natural selection drives transmission $\beta_k \to \infty$ and removal $\mu_k \to 0$, the standard approach is to constrain $R_{0,k}$ by invoking a trade-off such that increases in the transmission rate β_k will be accompanied by increases in the removal rate μ_k (Anderson and May 1982; Acevedo et al. 2019). If the increase in μ_k accelerates as β_k increases, natural selection will favor intermediate values of β_k and thus intermediate virulence (Keeling and Rohani 2008). Because pathogen strains with the optimal value of $R_{0,k}$ will outcompete all other strains, in this model strains can coexist only if they have the same value of $R_{0,k}$. Pathogen coexistence in a broad sense is therefore impossible in this model, as it often is in simple host-pathogen models (Keeling and Rohani 2008).

Equations (1)–(4) belong to a broad class of models that were originally constructed by adding host reproduction and nondisease death to the SIR model of Kermack and McKendrick (1927). To construct a seasonal model, we instead eliminate the host reproduction term $a(S + I_i + I_r + R)$ and the death terms δS, δI_i, δI_r, and δR from equations (1)–(4), thereby returning to the original Kermack-McKendrick model. We then embed the Kermack-McKendrick model in a set of difference equations that describe host reproduction and pathogen survival during the interepidemic period. Because the total fraction infected in our model is determined by the cumulative fraction infected with each pathogen strain, we replace the single removed class R in equation (4) with two removed classes Z_r and Z_i, representing the resident and the invader, respectively. Our epidemic model is then

$$\frac{dS}{dt} = -\beta_r SI_r - \beta_i SI_i, \quad (5)$$

$$\frac{dI_r}{dt} = \beta_r SI_r - \mu_r I_r, \quad (6)$$

$$\frac{dI_i}{dt} = \beta_i SI_i - \mu_i I_i, \quad (7)$$

$$\frac{dZ_r}{dt} = \mu_r I_r, \quad (8)$$

$$\frac{dZ_i}{dt} = \mu_i I_i. \tag{9}$$

Note that here and throughout we allow for two pathogen strains. Results from two-strain models cannot always be generalized to the case of multiple strains (Dieckmann 2002), but two-strain models nevertheless serve as a useful starting point (Alizon and Michalakis 2015).

When only the resident is present and the initial fraction infected with the resident is low, the density of the host at first changes very slowly, so that $S(0)$ is roughly constant. Under these conditions it is straightforward to solve equation (6) for the fraction infected with the resident at the beginning of the epidemic: $I_r(t) \approx I_r(0)\exp(\beta_r S(0) - \mu_r)$. An analogous equation holds when only the invader is present. Because at the beginning of an epidemic $S(0) \approx 1$, we can define the instantaneous relative fitness of the invader at the beginning of an epidemic as $\gamma_0 \equiv \lambda_{0,i}/\lambda_{0,r} \equiv (\beta_i - \mu_i)/(\beta_r - \mu_r)$, where $\lambda_{0,r}$ and $\lambda_{0,i}$ are the initial absolute fitnesses of the resident and the invader, respectively (note that $\lambda_{0,k}$ is sometimes referred to as "epidemic speed" [Dushoff and Park 2021] or the "epidemic growth rate" [Parag et al. 2021], symbolized as r_k; to avoid confusion with r for the resident, here we instead use λ). We use the subscript 0 to indicate that as in the definitions of $R_{0,r}$ and $R_{0,i}$, the definitions of γ_0, $\lambda_{0,r}$, and $\lambda_{0,i}$ hold only if $S \approx 1$, which is true only if $t \approx 0$.

Like the reproduction number $R_{0,i}$, the initial epidemic fitness $\lambda_{0,k}$ is calculated when the fraction susceptible $S(t) \approx 1$, so $\lambda_{0,k} = \beta_k - \mu_k$ is the difference between the number of new infections per unit time per infectious host minus the number of removals per unit time per infectious host and is thus the net number of new infections per unit time. As we will show, $\lambda_{0,r}$ and $\lambda_{0,i}$ are as important for understanding coexistence in seasonal environments as $R_{0,r}$ and $R_{0,i}$.

It is convenient to rescale time according to $\hat{t} \equiv \mu_r t$, so that time is measured in units of the average infectious life span of the resident strain r. It is also convenient to define the ratio of removal rates $u \equiv \mu_i/\mu_r$ and to replace β_k and μ_k for each pathogen strain with the reproductive numbers $R_{0,k} \equiv \beta_k/\mu_k$. If we then drop the hat from $\hat{t}$, we have a rescaled version of our epidemic model:

$$\frac{dS}{dt} = -R_{0,r}SI_r - uR_{0,i}SI_i, \tag{10}$$

$$\frac{dI_r}{dt} = R_{0,r}SI_r - I_r, \tag{11}$$

$$\frac{dI_i}{dt} = uR_{0,i}SI_i - uI_i, \tag{12}$$

$$\frac{dZ_r}{dt} = I_r, \tag{13}$$

$$\frac{dZ_i}{dt} = uI_i. \tag{14}$$

A key feature of single-epidemic SIR models is that eventually the fraction infected approaches zero, a phenomenon known as "epidemic burnout." Importantly, at epidemic burnout the fraction susceptible is often well above zero (Thieme 2003), as figure 1 illustrates. To

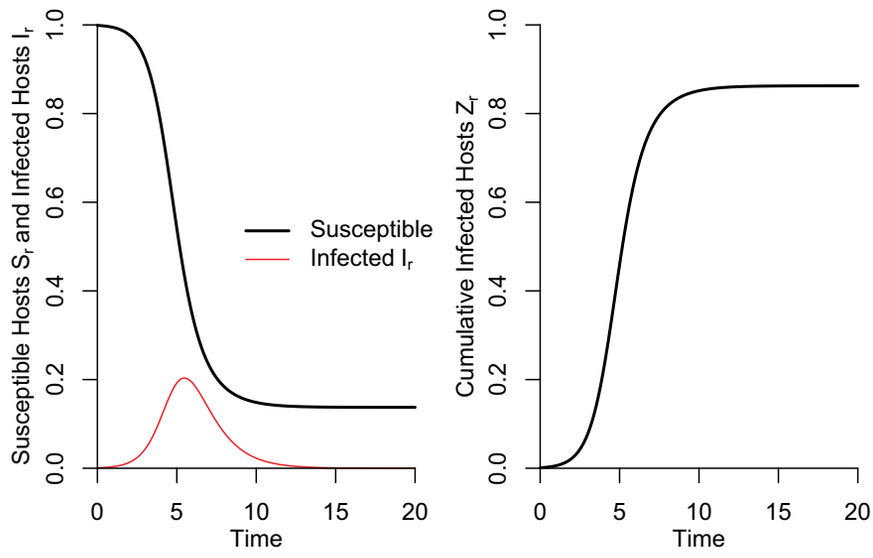

Figure 1: Dynamics of the single-strain SIR model, equations (10) and (11). Note that the final fraction susceptible is greater than zero at the end of the epidemic and thus at burnout. Here, the pathogen reproductive number $R_{0,r} = 2.3$.

understand this effect, Kermack and McKendrick (1927) derived an implicit expression for the cumulative fraction infected at burnout $Z_r(\infty)$:

$$1 - Z_r(\infty) = \exp(-R_{0,r}(S(0)Z_r(\infty) + I_r(0))). \quad (15)$$

As our notation implies, the burnout equation assumes that time $t \to \infty$, but as figure 1 illustrates $Z_r(\infty)$ can be quite close to its burnout value even if time t is not that large. Indeed, as we document in the discussion section, literature data suggest that epidemics of many animal and plant pathogens approach burnout every year.

In addition to providing a realistic summary of animal and plant epidemics in nature (Fuller et al. 2012), the burnout equation is useful because its analytical tractability and computational convenience allow for a deeper conceptual understanding of epidemics than can be provided by simulations alone. The equation's analytical tractability makes it possible to show, for example, that when the initial infection rate $I_r(0) \approx 0$, the equation has a nonzero solution $Z_r(\infty)$ only if $S(0) > 1/R_{0,r}$, so an epidemic can occur only if the fraction susceptible is above the threshold value of $1/R_{0,r}$. This is a version of the well-known threshold theorem of epidemiology (Kermack and McKendrick 1927).

The burnout equation's computational convenience is important because we can use the equation to calculate the fraction infected $Z_r(\infty)$ using a numerical root-finding routine, for example, the function uniroot() in the R programming language. It is also possible to approximate $Z_r(\infty)$ by numerically integrating the full model equations (10) and (11)—for example, by using the function ode() in R—but numerical root-finding routines require fewer lines of code and less run time. Moreover, the time that it takes for a model epidemic to approach burnout changes as the model parameters change, so using a differential equation solver to calculate $Z_r(\infty)$ requires either that we reset our choice of time interval for each parameter set or that we numerically integrate the model over a time interval that is long enough to assure that burnout occurs for essentially all parameter values. Changes in parameter values are, in contrast, a nonissue when we solve the burnout equation using a root-finding algorithm, and this computational tractability again allows for a deeper conceptual understanding of epidemics.

To illustrate how the computational convenience of the burnout equation improves our conceptual understanding, in figure 2 we use a numerical root-finding routine to plot the cumulative fraction infected at burnout $Z_r(\infty)$ versus both the initial fraction infected $S(0)$ and the reproductive number $R_{0,r}$. As the figure makes clear and as visual inspection of the burnout equation confirms, changes in $S(0)$ and $R_{0,r}$ have identical effects on $Z_r(\infty)$. The figure also illustrates the threshold effect, in that $Z_r(\infty)$ increases very sharply with $S(0)$ for $S(0) > 1/R_{r,0}$; for $S(0) < 1/R_{r,0}$, in contrast, $Z_r(\infty)$ is near zero unless $I_r(0) > 10^{-3}$. For values of $S(0)$ above the threshold, however, increases in $I_r(0)$ have very little effect on $Z_r(\infty)$.

Although an analogous burnout equation cannot be derived for the two-strain model equations (10)–(14), the burnout equation for the single-strain model is still fundamental

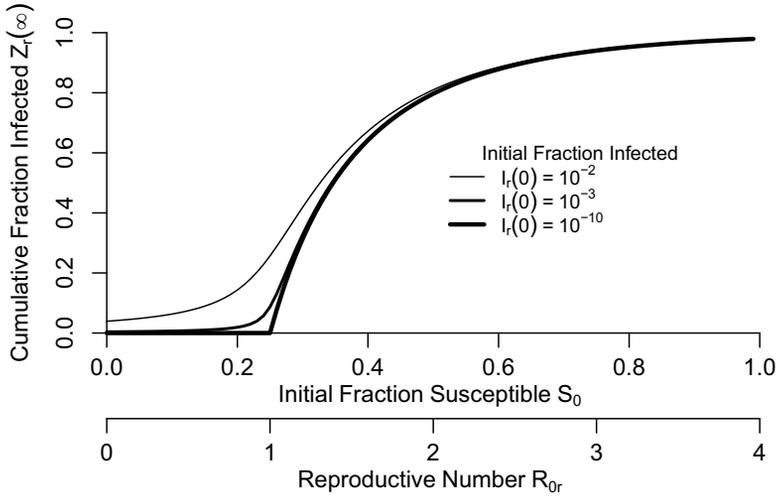

Figure 2: Effects of the reproductive number R_0 and the initial fractions susceptible S_0 and infected I_0 on the fraction infected at burnout. Here, we plot the cumulative fraction infected $Z_r(\infty)$, as calculated using the burnout equation (15), against the initial fraction susceptible $S(0)$ (upper horizontal axis) and the reproductive number $R_{0,r}$ (lower horizontal axis), for three different values of the initial fraction infected $I_r(0)$. The equivalence of the horizontal axes makes clear that changes in $S(0)$ and $R_{0,r}$ have equivalent effects on the cumulative fraction infected, while the low infection rates below the threshold of $1/R_{0,r} = 0.25$ demonstrate the importance of the threshold.

to our analyses. This is because an understanding of coexistence requires the use of invasion analysis, which assumes that the resident is at equilibrium before the invasion: we can therefore use the burnout equation to describe the resident's cumulative infection rate at the preinvasion equilibrium. Moreover, one of our key results is that we have derived a highly accurate approximation to the full two-pathogen model at the beginning of an invasion, and this approximation is nearly as analytically tractable and computationally convenient as the burnout equation. The burnout equation thus illustrates the analytic tractability and computational convenience that we strive for in our analyses.

Interepidemic Model. Because we assume that the host's population density is constant, we do not need an explicit term for host reproduction. To complete our model, we therefore need allow only for the interepidemic survival of each pathogen strain, which is equivalent to allowing for interepidemic transmission. Using n to indicate the host generation, our interepidemic model is then

$$S^{n+1}(0) = 1 - I_r^{n+1}(0) - I_i^{n+1}(0), \tag{16}$$

$$I_r^{n+1}(0) = W_r Z_r^n(\infty), \tag{17}$$

$$I_i^{n+1}(0) = W_i Z_i^n(\infty). \tag{18}$$

Here, $S^{n+1}(0)$ is the initial fraction susceptible during the epidemic in generation $n + 1$, which is equal to 1 minus the initial fraction infected with each pathogen strain, $I_r^{n+1}(0)$ and $I_i^{n+1}(0)$. The initial fraction infected with each pathogen strain is in turn proportional to the cumulative fraction infected by that strain in the previous generation; because the cumulative fractions infected are calculated at epidemic burnout, they are symbolized by $Z_r^n(\infty)$ and $Z_i^n(\infty)$, respectively. Note that at the beginning of each epidemic the cumulative fraction infected is by definition zero in both strains: $Z_r^n(0) = Z_i^n(0) = 0$. We also assume that infections in one epidemic can affect only the following epidemic, so that there are no multiyear effects.

The parameters W_r and W_i are the effective interepidemic survival rates for the two strains. Here, "effective" means that W_r and W_i allow for the possibility of higher or lower levels of susceptibility at the beginning of the epidemic relative to later in the epidemic. In the interaction between the spongy moth (*Lymantria dispar*, formerly known as the "gypsy moth") and its baculovirus as well as in some other interactions between insects and their baculoviruses, larvae are far smaller and thus more susceptible at the beginning of the epidemic than they are later in the epidemic, an effect that more than compensates for interepidemic pathogen mortality: W_r and W_i are therefore greater than 1 in such systems (Fleming-Davies and Dwyer 2015). In our analyses, we instead assume that $W_r, W_i \ll 1$ on the grounds that interepidemic survival is likely to be low in most host-pathogen systems, but we know of no reason why our results would not hold if $W_r, W_i > 1$.

Model Analyses: Overview

A useful approach to understanding pathogen coexistence is to first understand pathogen invasions, in which a pathogen strain invades a host population that is already occupied by another pathogen strain that has reached a stable equilibrium. If an invasion can occur at this single-strain equilibrium and if each strain can invade the other, then coexistence is effectively guaranteed. We can apply invasion analysis to our model because the single-strain version of the model has an equilibrium that is stable as long as the resident pathogen's reproductive number $R_{0,r} = \beta_r/\mu_r > 1$, a standard criterion in host-pathogen models (Keeling and Rohani 2008), and as long as the resident pathogen's interepidemic survival rate $W_r < 1$ (supplemental PDF), a biologically reasonable assumption. We therefore use invasion analysis to ask: Is coexistence possible at the single-strain equilibrium in our model?

The short answer is yes; in our model, a strain with high infectiousness during epidemics and low survival between epidemics can coexist with a strain with low infectiousness during epidemics and high survival between epidemics. The longer answer is that coexistence in our model would superficially appear to require large differences in phenotype between coexisting strains, and an initial analysis confirms that such large differences can indeed lead to coexistence: an invading strain with sufficiently high reproductive number $R_{0,i}$ can coexist with a resident strain if the invader's interepidemic survival rate W_i is sufficiently low. This initial analysis, however, follows classical analyses in considering only whether the invading pathogen can cause an epidemic when the epidemic of the resident strain has already reached its burnout equilibrium. We therefore refer to this type of invasion as an "epidemic-equilibrium invasion."

This focus on equilibrium behavior is an important limitation because an invasion can alternatively occur at the beginning of an epidemic, well before the resident strain's infection rate has reached its burnout equilibrium. Showing that such "epidemic-transient" invasions can occur required that we carry out a second, novel analysis that describes the dynamics of invasions during a transient window near the beginning of the resident's epidemic. This novel analysis shows that an invader with lower reproductive number $R_{0,i}$ than the resident can invade if its initial epidemic fitness $\lambda_{0,r}$ is larger than the epidemic fitness $\lambda_{0,i}$ of the resident. Such a pathogen can successfully invade because its relatively high $\lambda_{0,i}$ allows it to infect at least a few hosts early in the epidemic, before the fraction infected by the resident

has reached high levels. In this case, the invader must again have a higher interepidemic survival rate W_i than the resident, but the compensating effects of the invader's higher initial fitness $\lambda_{0,i}$ are strong enough that coexistence can occur even if the invader's phenotype is quite similar to the resident's phenotype. Epidemic-equilibrium and epidemic-transient invasions together allow pathogens to coexist over a wide range of parameters, and we therefore conclude that coexistence is likely in seasonal environments.

Because the two types of invasion occur under different circumstances, we discuss them separately. Understanding epidemic-transient invasions in particular requires an extensive rethinking of pathogen competition, which is why a novel type of analysis is required. In explaining our analyses, we therefore focus on the case of epidemic-transient invasions.

Epidemic-Equilibrium Invasions

As we explained earlier, when only one pathogen strain is present the fraction infected during the epidemic stops changing at epidemic burnout, which is an equilibrium of the epidemic model equations (1)–(4). An invasion can then occur if the product of the reproductive number of the invading strain $R_{0,i}$ and the resident's fraction susceptible at burnout $S^*(\infty)$ is greater than 1 (Newman 2005; Andreasen and Sasaki 2006):

$$S^*(\infty)R_{0,i} > 1. \tag{19}$$

Here, the asterisk refers to the single-strain equilibrium of the season-to-season model, while the infinity symbol emphasizes that $S^*(\infty)$ is calculated at burnout: $S^*(\infty)$ is thus the fraction susceptible at burnout when the resident is at its preinvasion equilibrium. Because the resident's epidemic has reached burnout, $S^*(\infty) = S^*(0)(1 - Z_r^*(\infty))$, where $S^*(0)$ is the fraction susceptible at the beginning of the epidemic and $Z_r^*(\infty)$ is the cumulative fraction infected at burnout, where both are calculated at the single-strain equilibrium. Epidemic-equilibrium invasions thus occur at epidemic burnout when the resident is at its multigenerational equilibrium.

Figure 2 shows that a single-strain epidemic can occur even if the pathogen's initial infection rate is extremely low, but it does not show that an epidemic that begins with a lower fraction infected takes longer to reach burnout than does an epidemic that begins with a higher fraction infected. This phenomenon is important for coexistence because if a high-infectiousness invader has a low interepidemic survival rate, then in each year after the invasion there will be a delay before the invader's infection rate reaches a high level. If this delay is long enough, the resident can have at least a modest epidemic before it is outcompeted by the invader. Figure 3 confirms that such a scenario can indeed lead to coexistence. Mutual invasion occurs because the reverse is also true; if the strain with high infectiousness and low interepidemic survival is instead the resident, then the delay in the resident's epidemic will allow an invader with low infectiousness and high survival to successfully invade (see the supplemental PDF for a figure showing this reverse case).

A simple explanation for this coexistence mechanism is that at the start of each epidemic, seasonality resets the fraction infected with each strain. In the epidemic that follows an invading strain with relatively low infectiousness but high interepidemic survival will be pushed toward extinction, but at the beginning of the next epidemic it will be restored to a relatively high frequency. If the invading strain instead has relatively high infectiousness but low interepidemic survival, then the resident will be pushed toward extinction during each epidemic, again before being restored to a relatively high frequency at the beginning of the next epidemic. Seasonality therefore allows for coexistence in our model because it alternately favors high-infectiousness strains and high-survival strains.

Epidemic-equilibrium invasions can thus allow for coexistence as long as the interepidemic survival rate of the more infectious strain is sufficiently small (fig. 3); indeed, the interepidemic survival rate of the more infectious strain can be vanishingly low as long it is not zero. Coexistence can in contrast be prevented if the interepidemic survival rate of the more infectious strain is relatively high. There is thus an upper limit on the survival rate of the more infectious strain above which coexistence is impossible, but there is no lower limit other than zero.

Because coexistence through epidemic-equilibrium invasions requires that the more infectious strain be able to cause an epidemic even though the less infectious strain has reached epidemic burnout, the reproductive numbers of the competing strains must in general be very different for an epidemic-equilibrium invasion to lead to coexistence. Coexistence through epidemic-equilibrium invasions thus requires that the competing strains have very different phenotypes; as we will show, however, coexistence through epidemic transients allows the two pathogen strains to have quite similar phenotypes.

Epidemic-Transient Invasions

Although the epidemic-equilibrium invasion criterion allows for the inherently transient nature of seasonal environments, the assumption that the resident's epidemic has reached its burnout equilibrium means that our analysis of the epidemic-equilibrium case is conceptually similar to the analysis used to derive the classical criterion $R_{0,i} > R_{0,r}$, as we mentioned. As figure 3 illustrates, however, an epidemic-equilibrium invasion can be successful even if the resident's

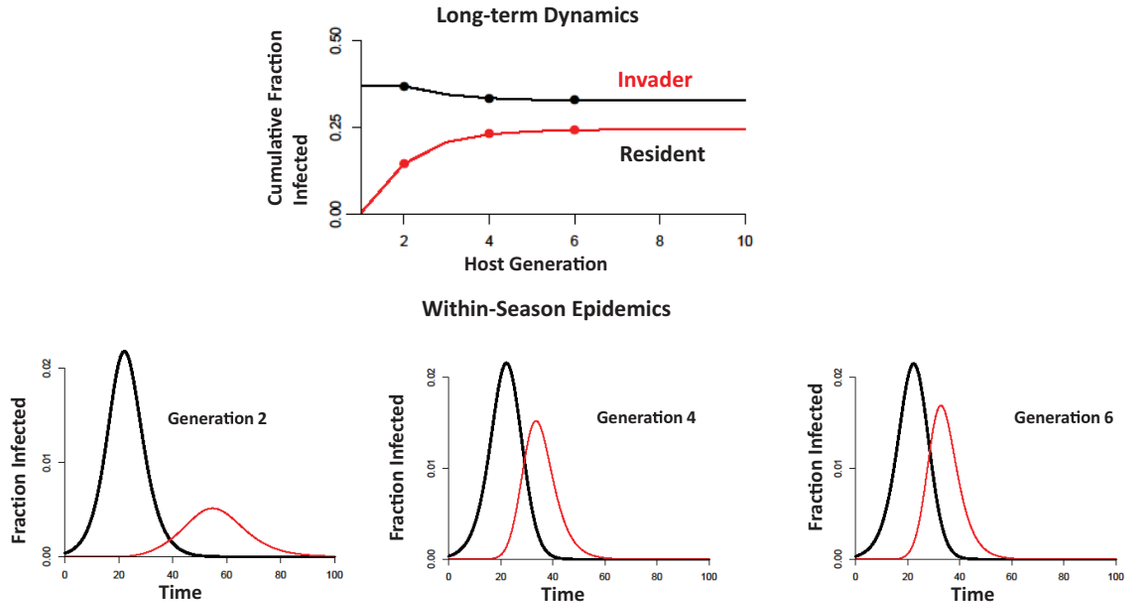

Figure 3: Simulation showing coexistence resulting from an epidemic-equilibrium invasion. At the beginning of the simulation, the resident's initial infection rate is equal to its single-strain equilibrium, while the invader's initial infection rate is 10^{-8}. The upper plot shows the cumulative infection rate of each pathogen at the end of the epidemic in each host generation, while the three lower plots show the epidemic dynamics in the three generations that are marked with solid circles in the upper plot. The infection rate of each pathogen changes during each epidemic, but once the coexistence equilibrium is reached the epidemic dynamics are the same in each generation. Here, the resident has transmission rate $\beta_r = 1.25$, removal rate $\mu_r = 1$, and interepidemic survival $W_r = 10^{-3}$, while the invader has transmission rate $\beta_i = 1.8$, removal rate $\mu_r = 1$, and interepidemic survival $W_r = 10^{-9}$. We therefore have $R_{0,r} = 1.25/1 < 1.8/1 = R_{0,i}$, so the invader has a higher reproductive number than the resident. Coexistence is thus possible because the invader's interepidemic survival rate is six orders of magnitude lower than the interepidemic survival rate of the resident.

epidemic has not yet reached burnout; indeed, such an invasion is even more likely to be successful than the epidemic-equilibrium invasion criterion indicates. This observation suggests that the transient dynamics of epidemics may also affect invasions. Our next step is therefore to consider how transient dynamics may modulate invasions and thus pathogen coexistence.

In figure 4, we show an epidemic-transient invasion in which an invader with low infectiousness and high interepidemic survival successfully invades and coexists with a resident strain with high infectiousness and low interepidemic survival. As the figure shows, this invasion occurs even though the resident's epidemic terminates the invader's epidemic in each generation; crucially, however, such terminations do not occur until the fraction infected by the invader has reached a high level. The delay between the beginning of the resident's epidemic and the termination of the invader's epidemic therefore provides a window of opportunity during which the invader can invade. If the resident's interepidemic survival rate is sufficiently low relative to the invader's interepidemic survival rate, the delay between the beginning of the resident's epidemic and the termination of the invader's epidemic will be large enough to ensure the success of the invasion.

Notably, the two pathogen strains in the epidemic-transient invasion shown in figure 4 have much more similar phenotypes than the two pathogen strains in the epidemic-equilibrium invasion shown in figure 3. Because in the epidemic-equilibrium case the reproductive number of the invader must be so much higher than the reproductive number of the resident, the invader rapidly terminates the epidemic of the resident in each generation, leading to rapid invasion and rapid convergence to the coexistence equilibrium. In the epidemic-transient case, in contrast, the invader and the resident have nearly equal competitive ability during the epidemic, so convergence to the coexistence equilibrium is quite slow.

It is important to emphasize that when we switch the parameters for the resident and the invader in figures 3 and 4, invasion and coexistence are still possible (supplemental PDF). This is because in both cases coexistence results from a trade-off between intraepidemic infectiousness

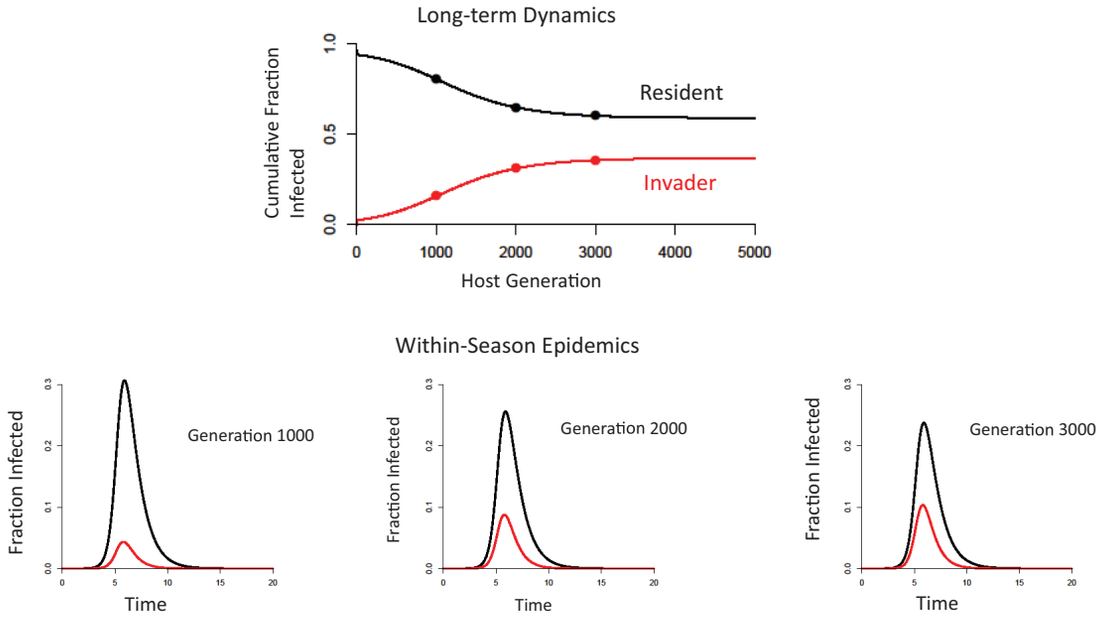

Figure 4: Simulation showing coexistence resulting from an epidemic-transient invasion. As in figure 3, the upper plot shows the cumulative infection rate of each pathogen at the end of the epidemic in each host generation, while the three lower plots show the epidemic dynamics in the generations that are marked with circles in the upper plot. Here, the resident has transmission rate $\beta_r = 3.5$, removal rate $\mu_r = 1$, and interepidemic survival rate $W_r = 1.1 \times 10^{-6}$, while the invader has transmission rate $\beta_i = 4$, removal rate $\mu_i = 1.3$, and interepidemic survival $W_i = 4.05 \times 10^{-7}$. In contrast to figure 3, the two pathogens thus have similar interepidemic survival rates, but the resident has a higher reproductive number than the invader, such that $R_{0,r} = 3.5/1 = 3.5 > 3.08 \approx 4/1.3 = R_{0,i}$, while the invader has a higher initial epidemic fitness than the resident, such that $\lambda_{0,i} = 4 - 1.3 = 2.7 > 2.5 = 3.5 - 1 = \lambda_{0,r}$. The invader's higher initial epidemic fitness thus counterbalances its lower reproductive number, leading to coexistence.

and interepidemic survival; in both cases a strain with low infectiousness and high survival therefore has an advantage early in the epidemic, while a strain with high infectiousness and low survival has an advantage late in the epidemic. In both cases coexistence thus occurs because the strain with low infectiousness but high interepidemic survival can cause infections early in the epidemic.

It is nevertheless true that epidemic-equilibrium invasions and epidemic-transient invasions occur for very different ranges of the model parameter values, implying that the two different types of invasion represent quantitatively different pathogen strategies. Because the model output for the two cases is qualitatively similar, however, and in particular because the time it takes to reach equilibrium provides only a rough indication of which case is which, simulations alone are insufficient for understanding the difference between the two cases. Understanding the difference thus instead required that we derive an analytic expression showing when epidemic-transient invasions are possible, analogous to the expression that we derived for epidemic-equilibrium invasions. Moreover, the epidemic-transient case is conceptually different from the epidemic-equilibrium case, so the equilibrium approach that we used in the epidemic-equilibrium case is insufficient for understanding the epidemic-transient case. To understand the epidemic-transient case, we therefore instead developed a new mathematical technique for analyzing pathogen invasions. Here, we use this technique to understand the conditions under which epidemic-transient invasions can occur.

Analyzing Epidemic-Transient Invasions. First, we consider the conditions under which the invader increases its initial infection rate $I_i(0)$ from one epidemic to the next, so that the invader is increasing in frequency. Because the invader's infection rate at the beginning of an epidemic is equal to its interepidemic survival W_i times the fraction infected in the previous epidemic $Z_i(\infty)$, the invader's frequency will only increase if

$$W_i Z_i(\infty) > I_i(0). \tag{20}$$

To use the above-described criterion to understand how transient epidemic dynamics allow for invasions, we must express the cumulative fraction infected by the invader $Z_i(\infty)$ in terms of the model parameters. To do this,

we recall that the rescaled SIR model equation (14) says that $dZ_i/dt = uI_i(t)$, where I_i is the instantaneous fraction infected by the invader and $u \equiv \mu_i/\mu_r$ is the ratio of invader μ_i and resident μ_r removal rates. Because $Z_i(0) = 0$, we can integrate both sides of equation (14) to get

$$Z_i(\infty) = u\int_0^\infty I_i(t)dt. \tag{21}$$

Although we cannot solve this integral outright, it is possible to approximate it in a way that allows us to derive an epidemic-transient invasion criterion. In the supplemental PDF, we show that this approximation is highly accurate in the sense that the output of the approximation is very close to the output of the full model equations (10)–(14).

To produce the approximation, we use a mathematical tool known as "multiple timescale analysis" (see the supplemental PDF). As its name implies, multiple timescale analysis allows us to consider the effects of pathogen competition over two distinct timescales within the epidemic; the short timescale at the beginning of the epidemic during which the invader can infect at least a few hosts, and the long timescale of the entire epidemic over which the invader's infection rate is driven to zero through competition with the resident (note that both timescales are much shorter than the timescale that includes the interepidemic period). By analyzing the epidemic separately over the two timescales, we can find conditions such that if the resident has a low initial fraction infected near the beginning of the epidemic, then the invader's advantage over the short timescale will outweigh its disadvantage over the long timescale.

A complication, however, is that rather than using t as a variable, our approximation uses the cumulative fraction infected by both strains $x(t) \equiv Z_i(t) + Z_r(t) = 1 - S(t)$ as a variable. The approximation is nevertheless useful because it allows us to calculate $Z_i(\infty)$; to do this, we change the variable of integration in equation (21) from t to x (supplemental PDF). We then have the following approximate expression for $Z_i(\infty)$:

$$Z_i(\infty) \approx I_i(0)I_r(0)^{-\gamma_0}u\left(\frac{R_{0,r}-1}{R_{0,r}}\right)^{\gamma_0} \times \int_0^{x_r^*(\infty)} \frac{x^{\gamma_0}\xi(x)}{(1-x)(R_{0,r}x + \log_e(1-x))}dx. \tag{22}$$

An additional complication is that the function $\xi(x)$ is calculated by solving the following differential equation:

$$\xi'(x) = \frac{\dfrac{u}{x-1} - \gamma_0\phi(x)}{R_{0,r} - 1 + x\phi(x)}\xi, \tag{23}$$

where we define $\phi(x) \equiv (x + \log_e(1-x))/x^2$.

Despite these complications, our approximate expression leads to a reasonably simple epidemic-invasion criterion in which invader fitness is expressed in terms of a short-term component and a long-term component (here "short term" and "long term" again refer to timescales during the epidemic). To generate this criterion, we first simplify our expression for invader fitness by defining the function

$$D_i(R_{0,r}, \gamma_0, u) \equiv u\left(\frac{R_{0,r}-1}{R_{0,r}}\right)^{\gamma_0} \times \int_0^{x_r^*(\infty)} \frac{x^{\gamma_0}\xi(x)}{(1-x)(R_{0,r}x + \log_e(1-x))}dx. \tag{24}$$

Here, the upper bound on the integral $x_r^*(\infty)$ is the fraction of hosts that are still susceptible at burnout when the resident is at its single-strain equilibrium.

Given this definition, we can rewrite the invader fitness equation (22) to produce an expression for $Z_i(\infty)/I_i(0)$, the increase in the invader's cumulative infection rate relative to its initial infection rate, in terms of components that represent invader fitness over short and long timescales:

$$\frac{Z_i(\infty)}{I_i(0)} \approx I_r(0)^{-\gamma_0}D_i(R_{0,r}, \gamma_0, u). \tag{25}$$

The short-term fitness component is $I_r(0)^{-\gamma_0}$, which is the initial fraction infected with the resident $I_r(0)$ raised to the power of the invader's initial relative fitness $\gamma_0 \equiv \lambda_{0,i}/\lambda_{0,r}$. The long-term fitness component is the function $D_i(R_{0,r}, \gamma_0, u)$, which represents the dynamical effects on the invader of competition with the resident.

To understand the relative importance of these two terms and their associated timescales, in figure 5 we plot the increase in season-to-season invader fitness $Z_i(\infty)/I_i(0)$ on the same axes as the short-timescale fitness component $I_r(0)^{-\gamma_0}$ and the long-timescale fitness component $D_i(R_{0,r}, \gamma_0, u)$, with the invader's initial relative fitness γ_0 on the horizontal axis. The figure shows that the short-timescale fitness component $I_r(0)^{-\gamma_0}$ increases very rapidly with increasing γ_0, as expected from visual inspection of the component. The term $D_i(R_{0,r}, \gamma_0, u)$, in contrast, decreases slowly with increasing γ_0. The dominant effects of the short-timescale term $I_r(0)^{-\gamma_0}$ thus cause small changes in relative initial invader fitness γ_0 to lead to large increases in the invader's season-to-season fitness $Z_i(\infty)/I_i(0)$; we therefore conclude that in an epidemic-transient invasion, the early stages of the epidemic largely determine the change in invader fitness. In the supplemental PDF, we show that the dominance of $I_r(0)^{-\gamma_0}$ holds for broad ranges of both the resident's reproduction number $R_{0,r}$ and the relative removal rate $u = \mu_i/\mu_r$.

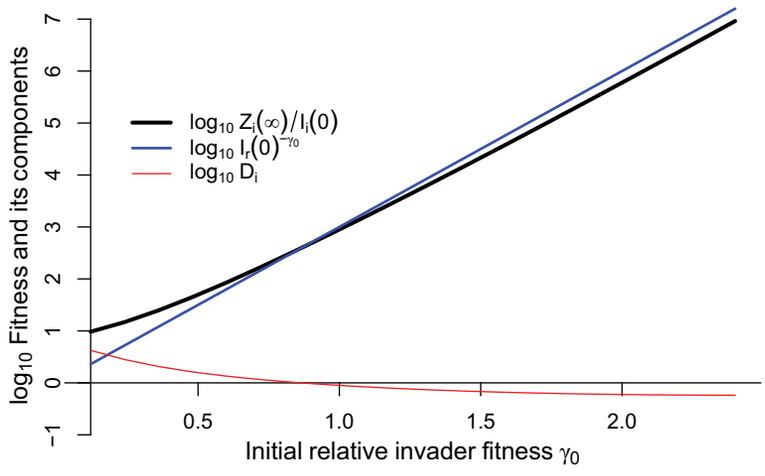

Figure 5: Effects of increasing initial relative invader fitness γ_0 on the invader's season-to-season increase in fitness $Z_i(\infty)/I_i(0)$. To understand the relative importance of the two components of invader fitness, we also plot the initial resident frequency raised to the power of the initial relative fitness $I_r(0)^{-\gamma_0}$ and the function that describes the dynamic effects of competition on the invader's fitness during the epidemic $D_i(R_{0,r}, \gamma_0, u)$. Here, the resident's reproductive number $R_{0,r} = 2.5$, the relative removal rate $u = \mu_i/\mu_r = 0.5$, and the resident's initial infection rate $I_r(0) = 10^{-5}$.

The strong effects of early epidemic dynamics on invader fitness are a result of the factors that determine the length of the delay between the start of the epidemic and the termination of the invader's epidemic by the resident. As figure 4 shows, during this delay the invader can infect at least a modest number of hosts; moreover, the delay is lengthened by reductions in the resident's initial infection rate $I_r(0)$. Reductions in $I_r(0)$ therefore increase invader fitness. The form of the short-timescale fitness component $I_r(0)^{-\gamma_0}$ then shows that an increase in initial relative invader fitness γ_0 is equivalent to a reduction in $I_r(0)$. Because reductions in $I_r(0)$ increase the delay between the start of the epidemic and the termination of the invader's epidemic by the resident, small increases in γ_0 lead to large increases in the invader's season-to-season fitness increase $Z_i(\infty)/I_i(0)$ (fig. 5). Increases in γ_0 thus increase the positive effect on the invader of the delay between the start of the invader's epidemic and its termination by the resident's epidemic.

Understanding why the term $D_i(R_{0,r}, \gamma_0, u)$ declines with increasing initial relative invader fitness γ_0 is more challenging. Mathematically, the decline occurs because of the term x^{γ_0} inside the integral in equation (24); because x is the cumulative fraction infected by both pathogens and is therefore less than 1, x^{γ_0} falls rapidly with increasing values of γ_0. Because the value of x during an initial invasion is almost entirely determined by the resident's epidemic and because the effects of γ_0 in $D_i(R_{0,r}, \gamma_0, u)$ are integrated over the entire epidemic, the decline in $D_i(R_{0,r}, \gamma_0, u)$ with increasing γ_0 represents the increase in the severity of the effects of competition on the invader that is due to increased relative invader fitness. Notably, however, these effects are far smaller than the effects of γ_0 on the term $I_r(0)^{-\gamma_0}$. The negative effects of increased pathogen competition that result from increases in γ_0 are thus trivial compared with the positive effects of the delay in the resident's epidemic that also result from increases in γ_0.

Why Transient Epidemic Dynamics Make Invasions More Likely. So far we have described epidemic-transient invasions only in terms of epidemic dynamics, but to fully understand epidemic-transient invasions we must understand how epidemic-transient invasions are affected by interepidemic dynamics. To do this, we recall that when the invasion begins the resident's initial infection rate $I_r(0)$ is at an equilibrium that is determined by the resident's interepidemic survival W_r and reproductive number $R_{0,r}$. This observation allows us to connect epidemic and interepidemic dynamics during epidemic-transient invasions, as follows.

First, recall that inequality (20) shows that for an epidemic-transient invasion to be successful, the invader's interepidemic survival rate W_i times the invader's season-to-season fitness $Z_i(\infty)$ must exceed the invader's fraction infected at the beginning of the epidemic $I_r(0)$: rearranging that inequality gives $1 < W_i Z_i(\infty)/I_i(0)$. We can then eliminate $Z_i(\infty)/I_i(0)$ from the inequality using our approximate expression from equation (25):

$$1 < W_i I_r(0)^{-\gamma_0} D_i(R_{0,r}, \gamma_0, u). \tag{26}$$

We can further eliminate $I_r(0)$ by recalling that at the resident-only equilibrium, $I_r^*(0) = W_r Z_r^*(\infty)$. Our epidemic-transient invasion criterion is then

$$1 < W_i (W_r Z_r^*(\infty))^{-\gamma_0} D_i(R_{0,r}, \gamma_0, u). \tag{27}$$

Understanding the conceptual implications of this criterion is easier if we first rewrite the cumulative infection rate of the resident at the preinvasion equilibrium as $Z_r^*(\infty) \equiv E_r(R_{0,r}, W_r)$, so that E_r represents the resident's cumulative infection rate at the resident-only equilibrium. After some rearranging, we have

$$\frac{\overbrace{E_r(R_{0,r}, W_r)^{\lambda_{0,i}}}^{\text{equilibrium infection rate of resident}}}{\underbrace{D_i(R_{0,r}, \lambda_{0,i}/\lambda_{0,r}, u)^{\lambda_{0,r}}}_{\text{dynamic effect of competition on invader}}} < \frac{\overbrace{W_i^{\lambda_{0,r}}}^{\text{interepidemic survival of invader}}}{\underbrace{W_r^{\lambda_{0,i}}}_{\text{interepidemic survival of resident}}}. \tag{28}$$

Because this criterion depends on the initial epidemic fitnesses of the invader $\lambda_{0,i}$ and the resident $\lambda_{0,r}$ as well as on the interepidemic survival rates of the invader W_i and the resident W_r, it connects the dynamics of the epidemic period to the dynamics of the interepidemic period. The criterion then shows that if $W_i > W_r$, it is easier for the invader to invade, but it also shows that high W_i can be counterbalanced by high $\lambda_{0,r}$, while high W_r can be counterbalanced by high $\lambda_{0,i}$. Likewise, the preinvasion equilibrium infection rate of the resident $E_r(R_{0,r}, W_r)$ is higher if W_r is higher (supplemental PDF), so high W_r makes it harder for the invader to invade; because $E_r(R_{0,r}, W_r)$ is less than 1, however, this effect is again counterbalanced by high $\lambda_{0,i}$. The equilibrium infection rate $E_r(R_{0,r}, W_r)$ is also higher if the resident has a high reproductive number $R_{0,r}$, but high $R_{0,r}$ can also be counterbalanced by high $\lambda_{0,i}$. The criterion thus shows that a high initial epidemic fitness in the invader can counterbalance a high reproductive number or a high interepidemic survival rate in the resident.

An important way in which epidemic-transient invasions differ from epidemic-equilibrium invasions is thus that epidemic-transient invasions depend on the relative values of the resident's reproductive number $R_{0,r}$ and the invader's initial epidemic fitness $\lambda_{0,i}$, whereas epidemic-equilibrium invasions depend on the relative values of the resident and invader reproductive numbers $R_{0,r}$ and $R_{0,i}$. Epidemic-transient invasions thus represent a novel mechanism by which pathogen invasions can occur.

To better understand the difference between the two types of invasion, recall that β_i and μ_i are the transmission rate and removal rate of the invader, respectively, and that the initial epidemic fitness of the invader is $\lambda_{0,i} \equiv \beta_i - \mu_i$, while the reproductive number of the invader is $R_{0,i} \equiv \beta_i/\mu_i$. The initial epidemic fitness of the invader $\lambda_{0,i}$ thus represents the net increase in the number of infections per unit time (assuming $\beta_i > \mu_i$, a necessary condition for an epidemic to occur), while the reproductive number of the invader $R_{0,i}$ instead represents the net increase in the number of infections per infectious life span. Proportional increases in β_i and μ_i, such that β_i and μ_i are multiplied by a number greater than 1, thus do not increase the invader's reproductive number $R_{0,i}$ but do increase the invader's initial epidemic fitness $\lambda_{0,i}$. Increasing $\lambda_{0,i}$ while keeping $R_{0,i}$ the same therefore increases the chance of a successful invasion because increases in $\lambda_{0,i}$ cause a more rapid accumulation of infections during the early stages of the epidemic.

Why Epidemic-Transient Invasions Make Coexistence More Likely. To understand how epidemic-transient invasions lead to coexistence, we consider the conditions under which mutual invasions are possible. To do this, we swap the roles of the resident and the invader by switching their subscripts, so that now i indicates the resident and r indicates the invader. Carrying out this switch in our epidemic-dynamic invasion inequality (28) produces an invasion expression for the former resident/current invader. We then have two epidemic-transient invasion criteria, which we combine to form a single coexistence criterion;

$$\begin{aligned} &\frac{E_r(R_{0,r}, W_r)^{\lambda_{0,i}}}{D_i(R_{0,r}, \lambda_{0,i}/\lambda_{0,r}, \mu_i/\mu_r)^{\lambda_{0,r}}} \\ &< \frac{W_i^{\lambda_{0,r}}}{W_r^{\lambda_{0,i}}} < \frac{D_r(R_{0,i}, \lambda_{0,r}/\lambda_{0,i}, \mu_r/\mu_i)^{\lambda_{0,i}}}{E_i(R_{0,i}, W_i)^{\lambda_{0,r}}}. \end{aligned} \tag{29}$$

Visual inspection of this coexistence criterion provides an initial understanding of why epidemic-transient invasions make coexistence likely in seasonal environments. The criterion shows first that if the invader has low initial epidemic fitness $\lambda_{0,i}$ but high interepidemic survival W_i while the resident has high initial epidemic fitness $\lambda_{0,r}$ but low interepidemic survival W_r, then the central term will have an intermediate value, increasing the chances of coexistence. The same is true if instead the invader combines high $\lambda_{0,i}$ with low W_i while the resident combines low $\lambda_{0,r}$ with high W_r.

The criterion further shows that the balance between equilibrium behavior and transient dynamics that is important for epidemic-transient invasions is also important for coexistence through epidemic-transient invasions. To emphasize this point, we rewrite our coexistence criterion in terms of the epidemic parameters alone, to identify epidemic parameters for which coexistence can occur for at least some values of the interepidemic survival rates W_r and W_i:

$$\frac{\overbrace{E_r(R_{0,r}, W_r)^{\lambda_{0,i}}}^{\text{equilibrial infection resident}}}{\underbrace{D_r(R_{0,i}, \lambda_{0,r}/\lambda_{0,i}, 1/u)^{\lambda_{0,r}}}_{\text{competition effects on resident}}} \times \frac{\overbrace{E_i(R_{0,i}, W_i)^{\lambda_{0,r}}}^{\text{equilibrial infection invader}}}{\underbrace{D_i(R_{0,r}, \lambda_{0,i}/\lambda_{0,r}, u)^{\lambda_{0,i}}}_{\text{competition effects on invader}}} < 1. \tag{30}$$

In this coexistence criterion, increases in the preinvasion equilibrium infection rates $E_r(R_{0,i}, W_i)$ and $E_r(R_{0,r}, W_r)$ due to increases in the reproductive numbers of the resident $R_{0,r}$ and the invader $R_{0,i}$ make coexistence less likely. These effects, however, can be counterbalanced by increases in the initial epidemic fitnesses of the invader $\lambda_{0,i}$ or the resident $\lambda_{0,r}$, which make coexistence more likely. Meanwhile, the functions $D_i(R_{0,r}, \lambda_{0,i}/\lambda_{0,r}, u)$ and $D_r(R_{0,i}, \lambda_{0,r}/\lambda_{0,i}, 1/u)$ decline slightly with increases in $\lambda_{0,i}$ and $\lambda_{0,r}$, making coexistence at least somewhat more likely as $\lambda_{0,i}$ and $\lambda_{0,r}$ increase.

Epidemic-transient invasions thus make coexistence more likely because of the counterbalancing effects of the reproductive number and the initial epidemic fitness of each pathogen strain on its competitor. Coexistence through burnout-equilibrium invasions, in contrast, depends on the reproduction number of each strain but not on the initial epidemic fitness of each strain. Epidemic-transient invasions thus allow for a different mechanism of coexistence than burnout-equilibrium invasions.

Quantifying the Likelihood of Coexistence in Seasonal Environments

Our invasion criteria have shown that epidemic-equilibrium and epidemic-transient invasions depend on the model parameters in very different ways. Because of these differences, the two types of invasion lead to coexistence for different ranges of the model parameters. Notably, however, model simulations cannot be used to distinguish these differences, and we therefore use our invasion criteria to map out the range of parameters for which coexistence occurs through each type of invasion.

As an initial illustration of the difference between the two types of invasion, we map coexistence as a function of the resident's reproductive number $R_{0,r}$ under each coexistence criterion. To map coexistence through epidemic-equilibrium invasions, we rewrite the epidemic-equilibrium invasion criterion, inequality (19), as

$$(1 - E_r(R_{0,r}, W_r))R_{0,i} > 1, \tag{31}$$

where $R_{0,i}$ is the invader's reproductive number and E_r is the resident's infection rate at burnout at the resident-only equilibrium, which is determined by the resident's reproductive number $R_{0,r}$ and its interepidemic survival W_r. Because $E_r(R_{0,r}, W_r)$ increases with increasing $R_{0,r}$, for a given value of $R_{0,i}$ there will be a maximum value of $R_{0,r}$ at which an invasion can occur. This maximum is the upper limit on $R_{0,r}$ for which an epidemic-equilibrium invasion can lead to coexistence for a given value of $R_{0,i}$.

To plot coexistence through epidemic-transient invasions, we first express the epidemic-transient coexistence inequality (29) in terms of the relative initial invader fitness $\gamma_0 = \lambda_{0,i}/\lambda_{0,r}$ and the ratio of removal rates $u = \mu_i/\mu_r$, and we plot the area between $D_i(R_{0,r}, \gamma_0, u)/(E_r(R_{0,r})^{\gamma_0}$ and $E_i(R_{0,i}, W_i)/D_r(R_{0,i}, 1/\gamma_0, 1/u)^{\gamma_0}$. Figure 6 then shows that compared with epidemic-equilibrium invasions, epidemic-transient invasions lead to coexistence for substantially larger values of the resident's reproductive number $R_{0,r}$. Epidemic-transient invasions can thus strongly increase the range of parameters for which coexistence is possible.

To show that coexisting pathogens can be more similar when coexistence occurs through epidemic-transient invasions than when it occurs through epidemic-equilibrium invasions, in figure 7 we map coexistence as a function of the instantaneous transmission rates of the resident β_r and the invader β_i. The figure then shows that the transmission

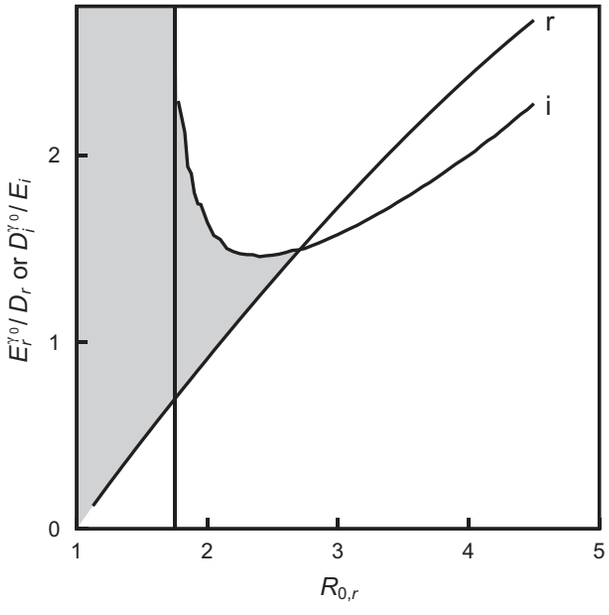

Figure 6: Effects of the resident's reproductive number $R_{0,r}$ on coexistence. The shaded area shows the range of values of $R_{0,r}$ for which there exist values of the interepidemic survival rates W_r and W_i that allow for coexistence. Here, the invader reproductive number $R_{0,i} = 3.5$ and the ratio of removal rates $u = \mu_i/\mu_r = 2.0$. The vertical line shows the maximum value of the resident transmission rate $R_{0,r} = 1.754$ that allows for epidemic-equilibrium invasions. For $R_{0,r} > 1.754$, coexistence can occur because of an epidemic-transient invasion; this range is found between the two curves.

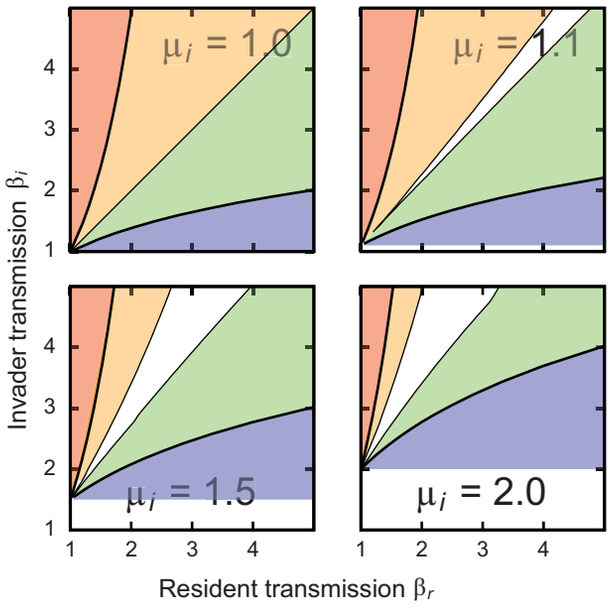

Figure 7: Range of invader and resident transmission rates for which coexistence is possible. Here, we show values of the instantaneous transmission rates β_r and β_i for which there exist combinations of interepidemic survival W_r and W_i that permit pathogen coexistence, for $\mu_r = 1$, and for a range of values of the invader's removal rate μ_i. In the white band across the bottom of the plots for which $\mu_i > 1$, coexistence is impossible because the invader's transmission rate β_i is so low that the invader's reproductive number $R_{0,i} = \beta_i/\mu_i < 1$; in this region, the invader is therefore unable to persist even in the absence of the resident. In the white areas around the 1:1 line, in contrast, coexistence is impossible because the invader and the resident are too similar. Coexistence then occurs in the colored areas to the upper left and the lower right. In the areas to the upper left, the invader has high infectiousness, so coexistence requires that the resident have high interepidemic survival; in the areas to the lower right, the situation is reversed, so that the resident has high infectiousness and the invader is required to have high survival. In the red/upper left areas and blue/lower right areas coexistence can occur through epidemic-equilibrium invasions, while in the yellow areas and green areas that are respectively adjacent to the red and blue areas coexistence can occur through epidemic-transient invasions. In the red and yellow areas the resident must have a higher interepidemic survival than that of the invader, so that $W_r > W_i$, while in the blue and green areas the invader must have a higher interepidemic survival than the resident, so that $W_i > W_r$.

rates that allow for coexistence through epidemic-transient invasions are closer to the 1:1 line than the transmission rates that allow for coexistence through epidemic-equilibrium invasions. When $\mu_i = \mu_r$, this effect is so strong that coexistence is possible for essentially all epidemic parameter values (remember that the effects of the interepidemic survival rates are not shown, so coexistence will be possible for only some interepidemic survival rates). Coexisting pathogen strains can thus have much more similar phenotypes when coexistence occurs through epidemic-transient invasions than when coexistence occurs through epidemic-equilibrium invasions. More generally, figure 7 shows that the total area over which coexistence can occur, whether through epidemic-transient or epidemic-equilibrium invasions, encompasses a broad range of parameter values. Pathogen coexistence is thus highly likely in seasonal environments.

To show how coexistence is affected by changes in the interepidemic survival rates W_r and W_i, we instead fix the epidemic parameters while mapping coexistence as a function of W_r and W_i. Figure 8 then shows that coexistence through epidemic-transient invasions is possible for broad ranges of W_r and W_i. Notably, coexistence requires differences in survival rates of an order of magnitude or more, and such differences must be larger when the relative removal rate $u = \mu_i/\mu_r$ is larger. Although these differences may seem large, estimates of interepidemic survival rates for 16 isolates of the spongy moth baculovirus vary over at least two orders of magnitude (Fleming-Davies

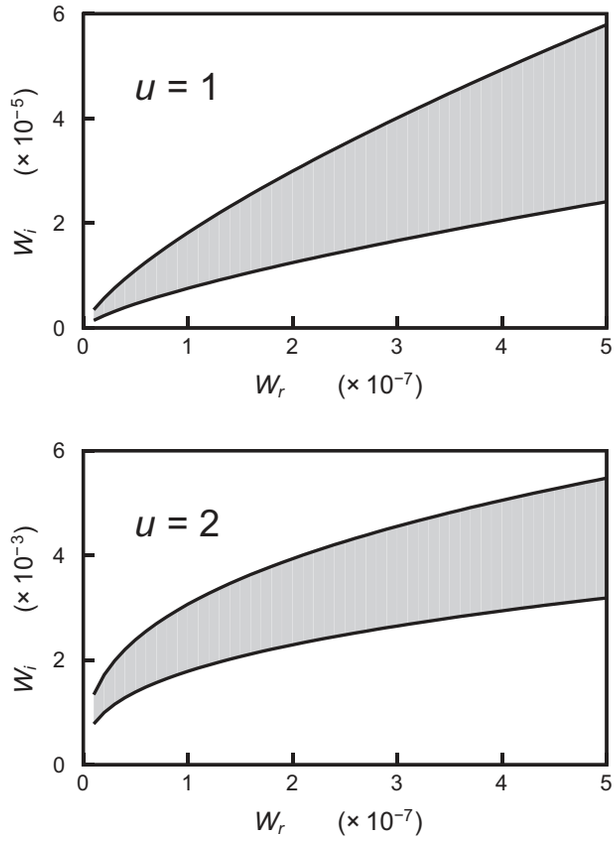

Figure 8: Combinations of interepidemic survival for the invader W_i and the resident W_r that allow for coexistence (shaded area). Here, $R_{0,r} = 3.5$, $R_{0,i} = 1.9$, and $u = 1, 2$. Notice the two-order-of-magnitude difference in scale on the W_i-axis between panels.

and Dwyer 2015): the differences in interepidemic survival rates necessary for coexistence in our model are thus consistent with observations of interepidemic survival in the field. Coexistence of isolates of the spongy moth baculovirus is also common in the field, supporting our overall conclusion that pathogen coexistence is likely in seasonal environments.

As we described earlier, coexistence through epidemic-equilibrium invasions can occur for vanishingly low values of the survival rate of the more infectious strain. There is, however, an upper limit above which coexistence is impossible; although we cannot write down an expression for this limit, in the supplemental PDF we use simulations to approximately quantify the limit. This approximate calculation shows that coexistence through epidemic-equilibrium invasions for the most part requires even larger differences in survival rates than does coexistence through epidemic-transient invasions. Given that coexistence through epidemic-equilibrium invasions invariably requires larger differences in transmission rates than does coexistence through epidemic-transient invasions (fig. 7), we conclude that coexistence through epidemic-equilibrium invasions generally requires that competing strains have more extreme phenotypes than does coexistence through epidemic-transient invasions.

Discussion

Our work shows that seasonal bouts of host reproduction and pathogen transmission can make it possible for a high-infectiousness/low-survival pathogen strain to coexist with a low-infectiousness/high-survival pathogen strain. Seasonality thus leads to pathogen coexistence because it allows pathogens to specialize on either the epidemic period or the interepidemic period, thereby allowing pathogens to pursue different strategies. In nonseasonal pathogen-competition models, in contrast, the epidemic and interepidemic periods are the same, so there is effectively only one possible strategy. Coexistence is therefore impossible in simple nonseasonal models (Dieckmann 2002).

The type of seasonality that we incorporated into our model has been observed in many host-pathogen systems in nature, and we therefore argue that our results are relevant to many different host-pathogen systems. Discrete bouts of host reproduction follow apparent epidemic burnout in viral (Fuller et al. 2012), fungal (Hajek 1999), and protozoan (Forbes et al. 2012) pathogens of insects and in viral (Honjo et al. 2020) and fungal (Penczykowski et al. 2015) pathogens of plants. Meanwhile, a slightly different pattern that is also consistent with our model occurs in many vertebrate-pathogen interactions, in which a low infection rate in the period leading up to the breeding season is followed by a spike in the infection rate due to the influx of new susceptible hosts that accompanies breeding. This pattern occurs in pestivirus of Pyrenean chamois, *Rupicapra pyrenaica pyrenaica* (Beaunée et al. 2015); classical swine fever in wild boars, *Sus scrofa* (Scherer et al. 2019); cowpox virus in field voles, *Microtus agrestis* (Begon et al. 2009); the respiratory pathogen *Bordetella bronchiseptica* (Pathak et al. 2011) and the myxoma virus (Dwyer et al. 1990) in the European rabbit, *Oryctolagus cuniculus*; white nose syndrome, *Pseudogymnoascus destructans*, in multiple species of bats (Langwig et al. 2015); Ebola and Marburg viruses in the Egyptian fruit bat, *Rousettus aegyptiacus* (Hayman 2015); avian flu in multiple species of dabbling ducks (Van Dijk et al. 2014; Lisovski et al. 2017); beak-and-feather virus disease of crimson rosellas, *Platycercus elegans* (Martens et al. 2020); and the pathogenic trematode *Ribeiroia ondatrae* in Pacific chorus frogs, *Pseudacris regilla* (McDevitt-Galles et al. 2020).

An infectiousness-survival trade-off is necessary for coexistence in our model, and it is therefore important to note that empirical support for pathogen fitness trade-offs is generally strong (Alizon et al. 2009; Leggett et al. 2013); a meta-analysis of 29 separate studies detected statistically significant relationships between pathogen replication and virulence and between pathogen replication and transmission (Acevedo et al. 2019). Although trade-offs between infectiousness and survival have been studied much less intensively than trade-offs that directly involve pathogen replication, an infectiousness/survival trade-off has been documented in the baculovirus of the spongy moth (Fleming-Davies and Dwyer 2015) and in multiple fungal pathogens of plants (van den Berg et al. 2010; Penczykowski et al. 2015; Suffert et al. 2015).

A related point is that a trade-off between within-epidemic infectiousness and between-epidemic survival is analogous to a competition-colonization trade-off. Competition-colonization trade-offs are typically invoked in the context of spatial dynamics, such that two organisms repeatedly colonize patches that are episodically vacated by disturbances. Coexistence can then occur because a species with high dispersal can briefly colonize vacant patches before being displaced by a second species with greater competitive ability within a patch (Bolker and Pacala 1999). In our case, high interepidemic survival analogously allows a competitor to briefly "colonize" a window in time before being displaced by a competitor with greater competitive ability within an epidemic.

In addition to supporting our model's assumptions, the empirical literature also supports our model's conclusions. Field studies have shown that both seasonality (Altizer et al. 2006; Filion et al. 2020; Poulin 2020) and pathogen coexistence (Hellard et al. 2015; Betts et al. 2016; Fountain-Jones et al. 2018) are common in animal-pathogen and plant-pathogen interactions in nature. Our model thus

provides a simple and empirically supported explanation for a widely observed pattern.

Our coexistence criteria greatly reduced the computational difficulty of mapping parameter space and thus made it easier to map the range of parameters over which coexistence occurs. If we had instead used the full model to carry out this mapping, we would have had to numerically integrate five differential equations over long time intervals that could not be specified in advance while iterating three difference equations until they reached either a coexistence equilibrium or a single-pathogen equilibrium, as in figures 3 and 4. Indeed, it is because of these constraints that our quantification of the upper limit on interepidemic survival of the more infectious strain (supplemental PDF) provides only a rough approximation. Mapping parameter space using the analytic expressions produced by our multiple timescale analysis, in contrast, required only that we numerically integrate two differential equations over a short fixed interval, leading to a highly accurate mapping.

The larger significance of our coexistence criteria, however, is that they led to our second main result: that coexistence occurs through two different types of invasions and that the two different types of invasion occur in adjacent but different regions of parameter space. Epidemic-equilibrium invasions, which occur if an invader can cause an epidemic after the resident's epidemic has reached the burnout equilibrium, require that the two competing strains have quite different phenotypes. Epidemic-transient invasions, which occur if an invader can take advantage of a transient period at the beginning of the epidemic when the resident's fraction infected is low, allow the two competing strains to have quite similar phenotypes. Coexistence in the two cases is qualitatively similar because in both cases a less infectious strain can increase its infection rate at the beginning of the epidemic before being outcompeted by the more infectious strain. In quantitative terms, however, the strategies of the less infectious strains differ very strongly between the two cases; moreover, simulations alone would not have revealed this distinction.

Understanding the difference between the two types of invasion thus required that we derive a coexistence criterion that would allow us to quantify the range of parameters over which coexistence occurs through each type of invasion. The difference in these parameter ranges is important first because it makes clear that pathogen invasions in seasonal environments can be understood only by considering both equilibrium epidemic behavior and transient epidemic behavior, second because the occurrence of epidemic-transient invasions greatly expands the total range of parameters over which coexistence occurs, and third because coexistence through epidemic transients allows pathogen strains to be much more similar than does coexistence through epidemic-equilibrium invasions. The most important feature of our invasion criteria is thus that they provide a conceptually novel perspective on pathogen coexistence.

The argument that a pathogen's initial epidemic fitness can be as useful for understanding pathogen invasions as its reproductive number was also made in a study of SARS-CoV-2 variants (Park et al. 2021); that work, however, focused on short-term dynamics and thus did not consider how initial epidemic fitness affects long-term pathogen coexistence. Our work therefore appears to be the first to disentangle the relative importance of equilibrium behavior and transient dynamics in long-term pathogen coexistence. Epidemic-transient invasions may thus represent an overlooked mechanism by which pathogens coexist in nature.

As we described, the classical approach to pathogen coexistence is to consider only whether invasion can occur when one strain is at its single-strain equilibrium (Dieckmann 2002). Although we have shown that in seasonal environments this equilibrium approach must further account for differences in interepidemic survival, otherwise the approach is the same as in the nonseasonal case. By considering transient dynamics, however, we have shown that pathogen competition in seasonal environments can alternatively be determined by a balance between the reproductive numbers of the resident $R_{0,r}$ and the invader $R_{0,i}$ on the one hand and the initial epidemic fitnesses of the resident $\lambda_{0,r}$ and the invader $\lambda_{0,i}$ on the other hand. The analysis that produced this result is sufficiently different from classical equilibrium-based analyses that carrying out the analysis required a significant conceptual leap.

Although for convenience we have described the competing pathogens in our model as following one of two strategies, such that one pathogen has high infectiousness and low interepidemic survival and the other has low infectiousness and high interepidemic survival, this wording implies a false dichotomy; in reality, our model allows for a continuum of strategies, such that different strategies take advantage of the window of opportunity near the beginning of the epidemic to different degrees. It is therefore more accurate to say that our model allows for coexistence through multiple mechanisms. The question of whether these multiple mechanisms can lead to the coexistence of more than two strains is then an avenue for further research.

A related point is that, as we described, a previous study used an evolutionary branching analysis to similarly argue that seasonality can lead to coexistence (Hamelin et al. 2011); because evolutionary branching analyses explicitly consider a continuum of strategies, a similar approach may be useful for understanding the evolutionary dynamics of coexistence in our model. An important caveat, however, is that evolutionary branching analyses assume that

phenotypic changes are small, whereas observations of the evolution of virulence of the myxoma virus of European rabbits, *O. cuniculus* (Dwyer et al. 1990; Kerr et al. 2017), and the evolution of higher transmission in the SARS-CoV-2 virus of humans (Kistler et al. 2022) suggest that pathogen evolution often leads to large phenotypic changes.

Although both our model and the model of Hamelin et al. (2011) lead to the conclusion that seasonality can allow for pathogen coexistence, the model of van den Berg et al. (2010) instead leads to the conclusion that seasonality cannot allow for pathogen coexistence. This difference is apparently due to differences in the assumptions that the models make about how infections during one epidemic affect the start of the next epidemic. In our model, the fraction infected at the beginning of an epidemic is determined by the cumulative fraction infected during the previous epidemic, while in the van den Berg et al. model the fraction infected at the beginning of an epidemic is determined by the fraction infected at the time when the previous epidemic ended. Like the van den Berg et al. model, the Hamelin et al. model assumes that what matters is the fraction infected at the time when the previous epidemic ended, but the Hamelin et al. model also includes a single additional round of infection before the next epidemic begins. In our model and in the Hamelin et al. model, infections during the epidemic period thus have a bigger effect on the infection rate at the beginning of the next epidemic than in the van den Berg et al. model, so strains with high interepidemic survival in the former two models have a bigger advantage, making coexistence more likely. Our model's assumption is supported at least qualitatively by the literature on a wide range of host-pathogen systems (Thompson and Scott 1979; Murray and Elkinton 1989; Hajek 1999; Penczykowski et al. 2015; Suffert et al. 2015; Becker et al. 2020; Honjo et al. 2020), but Hamelin et al. and van den Berg et al. similarly argue that their models' assumptions are supported qualitatively by literature on at least some plant-pathogen systems. The existing literature therefore appears to be insufficient to determine which of the models is most general and realistic. Part of the problem is that empirical tests of model assumptions about interepidemic survival are extremely rare (but see Fleming-Davies and Dwyer 2015), so such tests are an important future direction.

In arguing for the importance of seasonality we are not arguing against population structure as a mechanism of pathogen coexistence. Indeed, in previous work with colleagues we argued that population structure, in the form of differences in the level of variation in host susceptibility to different pathogen strains, a type of genotype-by-genotype interaction, helps to explain coexistence of strains of the spongy moth baculovirus (Fleming-Davies et al. 2015). That work nevertheless suggested that a trade-off between within-epidemic infectiousness and interepidemic survival could lead to coexistence, motivating the work that we present here. In analyzing the effects of seasonality, our intent is therefore to understand the importance of a mechanism for which we have supporting data from a host-pathogen system in nature; although population structure almost certainly enhances the likelihood of coexistence in the spongy moth-baculovirus system, the importance of seasonality as a mechanism that allows for pathogen coexistence in that system or in any other host-pathogen system has not been widely recognized. Moreover, by showing that seasonality can provide an explanation for pathogen coexistence when population structure is unimportant, we have shown that seasonality may explain coexistence for host-pathogen systems in which population structure plays little to no role. A key conclusion of our work is thus that population structure is not necessary for pathogen coexistence.

From this perspective, it is important to note that our multiple-timescale analysis is sufficiently general that it may be useful for understanding systems in which both seasonality and population structure are important. In such cases, our method of analysis should again make it possible to write down an approximate expression for the fraction infected (Gart 1968; Andreasen 2003). In future work we will therefore apply our analysis to understanding the combined effects of seasonality and population structure on pathogen coexistence, thereby achieving a more general understanding of the role of seasonality in mediating pathogen coexistence. More immediately, the analysis could be useful in understanding the dynamics of pathogen coexistence in the seasonal plant-pathogen models of van den Berg et al. (2010) and Hamelin et al. (2017) as well as in the seasonal sheep-pathogen model of Roberts and Heesterbeek (1998).

By showing that pathogen coexistence is a likely outcome in seasonal environments, we have extended previous results showing that seasonality and host evolution play key roles in host-pathogen population cycles (Páez et al. 2017; Dwyer et al. 2022). We therefore argue that seasonality is of general importance in modulating the roles of both pathogen competition and natural selection in host-pathogen interactions and thus that host-pathogen models that allow for seasonal bouts of transmission and host reproduction provide an important tool for understanding the evolutionary ecology of host-pathogen interactions.

Acknowledgments

V.A. was supported by grant 8020-00284 from the Danish Natural Science Research Council and by the Carlsberg Foundation, Semper Ardens Research Project (grant CF20-0046). G.D. was supported by Ecology and Evolution

of Infectious Diseases (EEID) grant DEB-2109774 from the US National Science Foundation.

Statement of Authorship

V.A. conceived of the project, proved the key results, and wrote important pieces of the code. G.D. wrote the more obvious pieces of code and wrote most of the text, with a great deal of help from V.A.

Data and Code Availability

The code is available on Zenodo (https://zenodo.org/badge/latestdoi/348009397; Andreasen and Dwyer 2021) and in G.D.'s GitHub repository (https://github.com/gregvirus2/AndreasenDwyerSeasonalityAndPathogenCoexistence).

Literature Cited

Acevedo, M. A., F. P. Dillemuth, A. J. Flick, M. J. Faldyn, and B. D. Elderd. 2019. Virulence-driven trade-offs in disease transmission: a meta-analysis. Evolution 73:636–647.

Albery, G. F., F. Kenyon, A. Morris, S. Morris, D. H. Nussey, and J. M. Pemberton. 2018. Seasonality of helminth infection in wild red deer varies between individuals and between parasite taxa. Parasitology 145:1410–1420.

Alizon, S., A. Hurford, N. Mideo, and M. Van Baalen. 2009. Virulence evolution and the trade-off hypothesis: history, current state of affairs and the future. Journal of Evolutionary Biology 22:245–259.

Alizon, S., and Y. Michalakis. 2015. Adaptive virulence evolution: the good old fitness-based approach. Trends in Ecology and Evolution 30:248–254.

Altizer, S., A. Dobson, P. Hosseini, P. Hudson, M. Pascual, and P. Rohani. 2006. Seasonality and the dynamics of infectious diseases. Ecology Letters 9:467–484.

Anderson, R. M., and R. M. May. 1982. Coevolution of hosts and parasites. Parasitology 85:411–426.

Andreasen, V. 2003. Dynamics of annual influenza A epidemics with immuno-selection. Journal of Mathematical Biology 46:504–536.

Andreasen, V., and G. Dwyer. 2021. Code from: Seasonality and the coexistence of pathogen strains. American Naturalist, Zenodo, https://zenodo.org/badge/latestdoi/348009397.

Andreasen, V., and A. Pugliese. 1995. Pathogen coexistence induced by density dependent host mortality. Journal of Theoretical Biology 177:159–165.

Andreasen, V., and A. Sasaki. 2006. Shaping the phylogenetic tree of influenza by cross-immunity. Theoretical Population Biology 70:164–173.

Beaunée, G., E. Gilot-Fromont, M. Garel, and P. Ezanno. 2015. A novel epidemiological model to better understand and predict the observed seasonal spread of pestivirus in *Pyrenean chamois* populations. Veterinary Research 46:86.

Becker, D. J., E. D. Ketterson, and R. J. Hall. 2020. Reactivation of latent infections with migration shapes population-level disease dynamics. bioRxiv, https://doi.org/10.1101/2020.05.12.091736.

Begon, M., S. Telfer, M. J. Smith, S. Burthe, S. Paterson, and X. Lambin. 2009. Seasonal host dynamics drive the timing of recurrent epidemics in a wildlife population. Proceedings of the Royal Society B 276:1603–1610.

Betts, A., C. Rafaluk, and K. C. King. 2016. Host and parasite evolution in a tangled bank. Trends in Parasitology 32:863–873.

Bolker, B. M., and S. W. Pacala. 1999. Spatial moment equations for plant competition: understanding spatial strategies and the advantages of short dispersal. American Naturalist 153:575–602.

Bremermann, H. J., and H. Thieme. 1989. A competitive exclusion principle for pathogen virulence. Journal of Mathematical Biology 27:179–190.

Briggs, J., K. Dabbs, M. Holm, J. Lubben, R. Rebarber, B. Tenhumberg, and D. Riser-Espinoza. 2010. Structured population dynamics: an introduction to integral modeling. Mathematics Magazine 83:243–257.

Buonomo, B., N. Chitnis, and A. d'Onofrio. 2018. Seasonality in epidemic models: a literature review. Ricerche di Matematica 67:7–25.

Clay, P. A., K. Dhir, V. H. Rudolf, and M. A. Duffy. 2019. Within-host priority effects systematically alter pathogen coexistence. American Naturalist 193:187–199.

Cory, J. S., and J. H. Myers. 2003. The ecology and evolution of insect baculoviruses. Annual Reviews of Ecology and Systematics 34:239–272.

Dieckmann, U. 2002. Adapative dynamics of pathogen-host interactions. Pages 39–59 *in* U. Dieckmann, K. Sigmund, and H. Metz, eds. Adaptive dynamics of infectious diseases: in pursuit of virulence management. Cambridge University Press, Cambridge.

Dorélien, A. M., S. Ballesteros, and B. T. Grenfell. 2013. Impact of birth seasonality on dynamics of acute immunizing infections in sub-Saharan Africa. PLoS ONE 8:e75806.

Dushoff, J., and S. W. Park. 2021. Speed and strength of an epidemic intervention. Proceedings of the Royal Society B 288:20201556.

Dwyer, G., S. A. Levin, and L. Buttel. 1990. A simulation-model of the population-dynamics and evolution of myxomatosis. Ecological Monographs 60:423–447.

Dwyer, G., J. R. Mihaljevic, and V. Dukic. 2022. Can eco-evo theory explain population cycles in the field? American Naturalist 199:108–125.

Filion, A., A. Eriksson, F. Jorge, C. N. Niebuhr, and R. Poulin. 2020. Large-scale disease patterns explained by climatic seasonality and host traits. Oecologia 194:723–733.

Fleming-Davies, A. E., V. Dukic, V. Andreasen, and G. Dwyer. 2015. Effects of host heterogeneity on pathogen diversity and evolution. Ecology Letters 18:1252–1261.

Fleming-Davies, A. E., and G. Dwyer. 2015. Phenotypic variation in overwinter environmental transmission of a baculovirus and the cost of virulence. American Naturalist 186:797–806.

Forbes, M. R., J. J. Mlynarek, J. Allison, and K. R. Hecker. 2012. Seasonality of gregarine parasitism in the damselfly, *Nehalennia irene*: understanding unimodal patterns. Parasitology Research 110:245–250.

Fountain-Jones, N. M., W. D. Pearse, L. E. Escobar, A. Alba-Casals, S. Carver, T. J. Davies, S. Kraberger, et al. 2018. Towards an eco-phylogenetic framework for infectious disease ecology. Biological Reviews 93:950–970.

Fuller, E., B. D. Elderd, and G. Dwyer. 2012. Pathogen persistence in the environment and insect-baculovirus interactions: disease-density thresholds, epidemic burnout, and insect outbreaks. American Naturalist 179:E70–E96.

Gart, J. J. 1968. The mathematical analysis of an epidemic with two kinds of susceptibles. Biometrics 24:557–565.

Gillespie, J. H. 1975. Natural selection for resistance to epidemics. Ecology 56:493–495.

Hajek, A. E. 1999. Pathology and epizootiology of *Entomophaga maimaiga* infections in forest lepidoptera. Microbiology and Molecular Biology Reviews 63:814–835.

Hamelin, F. M., M. Castel, S. Poggi, D. Andrivon, and L. Mailleret. 2011. Seasonality and the evolutionary divergence of plant parasites. Ecology 92:2159–2166.

Hamelin, F. M., F. M. Hilker, T. A. Sun, M. J. Jeger, M. R. Hajimorad, L. J. Allen, and H. R. Prendeville. 2017. The evolution of parasitic and mutualistic plant-virus symbioses through transmission-virulence trade-offs. Virus Research 241:77–87.

Havarua, Z., W. C. Turner, and J. K. Mfune. 2014. Seasonal variation in foraging behaviour of plains zebra (*Equus quagga*) may alter contact with the anthrax bacterium (*Bacillus anthracis*). Canadian Journal of Zoology 92:331–337.

Hayman, D. T. 2015. Biannual birth pulses allow filoviruses to persist in bat populations. Proceedings of the Royal Society B 282:20142591.

Hellard, E., D. Fouchet, F. Vavre, and D. Pontier. 2015. Parasite-parasite interactions in the wild: how to detect them? Trends in Parasitology 31:640–652.

Honjo, M. N., N. Emura, T. Kawagoe, J. Sugisaka, M. Kamitani, A. J. Nagano, and H. Kudoh. 2020. Seasonality of interactions between a plant virus and its host during persistent infection in a natural environment. ISME Journal 14:506–518.

Hosseini, P. R., A. A. Dhondt, and A. Dobson. 2004. Seasonality and wildlife disease: how seasonal birth, aggregation and variation in immunity affect the dynamics of *Mycoplasma gallisepticum* in house finches. Proceedings of the Royal Society B 271:2569–2577.

Hunter, A. F. 1995. Ecology, life history and phylogeny of outbreak and nonoutbreak species. Pages 41–64 *in* N. Cappuccino and P. Price, eds. Population dynamics: new approaches and synthesis. Academic Press, New York.

Keeling, M. J., and P. Rohani. 2008. Modeling infectious diseases in humans and animals. Princeton University Press, Princeton, NJ.

Kermack, W., and A. McKendrick. 1927. A contribution to the mathematical theory of epidemics. Proceedings of the Royal Society A 115:700–721.

Kerr, P. J., I. M. Cattadori, J. Liu, D. G. Sim, J. W. Dodds, J. W. Brooks, M. J. Kennett, E. C. Holmes, and A. F. Read. 2017. Next step in the ongoing arms race between myxoma virus and wild rabbits in Australia is a novel disease phenotype. Proceedings of the National Academy of Sciences of the USA 114:9397–9402.

Kistler, K. E., J. Huddleston, and T. Bedford. 2022. Rapid and parallel adaptive mutations in spike S1 drive clade success in SARS-CoV-2. Cell Host and Microbe 30:545–555.

Langwig, K. E., W. F. Frick, R. Reynolds, K. L. Parise, K. P. Drees, J. R. Hoyt, T. L. Cheng, T. H. Kunz, J. T. Foster, and A. M. Kilpatrick. 2015. Host and pathogen ecology drive the seasonal dynamics of a fungal disease, white-nose syndrome. Proceedings of the Royal Society B 282:20142335.

Leggett, H. C., A. Buckling, G. H. Long, and M. Boots. 2013. Generalism and the evolution of parasite virulence. Trends in Ecology and Evolution 28:592–596.

Levin, S., and D. Pimentel. 1981. Selection of intermediate rates of increase in parasite-host systems. American Naturalist 117:308–315.

Lion, S., V. A. Jansen, and T. Day. 2011. Evolution in structured populations: beyond the kin versus group debate. Trends in Ecology and Evolution 26:193–201.

Lisovski, S., B. J. Hoye, and M. Klaassen. 2017. Geographic variation in seasonality and its influence on the dynamics of an infectious disease. Oikos 126:931–936.

Lively, C. M., and M. F. Dybdahl. 2000. Parasite adaptation to locally common host genotypes. Nature 405:679–681.

Martens, J. M., H. S. Stokes, M. L. Berg, K. Walder, and A. T. Bennett. 2020. Seasonal fluctuation of beak and feather disease virus (BFDV) infection in wild crimson rosellas (*Platycercus elegans*). Scientific Reports 10:7894.

May, R. M. 1985. Regulation of populations with nonoverlapping generations by microparasites: a purely chaotic system. American Naturalist 125:573–584.

McDevitt-Galles, T., W. E. Moss, D. M. Calhoun, and P. T. Johnson. 2020. Phenological synchrony shapes pathology in host-parasite systems. Proceedings of the Royal Society B 287: 20192597.

Messinger, S. M., and A. Ostling. 2009. The consequences of spatial structure for the evolution of pathogen transmission rate and virulence. American Naturalist 174:441–454.

Mihaljevic, J. R., J. T. Hoverman, and P. T. Johnson. 2018. Co-exposure to multiple ranavirus types enhances viral infectivity and replication in a larval amphibian system. Diseases of Aquatic Organisms 132:23–35.

Mordecai, E. A., K. Gross, and C. E. Mitchell. 2016. Within-host niche differences and fitness trade-offs promote coexistence of plant viruses. American Naturalist 187:E13–E26.

Murray, K. D., and J. S. Elkinton. 1989. Environmental contamination of egg masses as a major component of transgenerational transmission of gypsy-moth nuclear polyhedrosis-virus (LdMNPV). Journal of Invertebrate Pathology 53:324–334.

Newman, M. E. J. 2005. Threshold effects for two pathogens spreading on a network. Physical Review Letters 95:108701.

Páez, D. J., V. Dukic, J. Dushoff, A. Fleming-Davies, and G. Dwyer. 2017. Eco-evolutionary theory and insect outbreaks. American Naturalist 189:616–629.

Parag, K. V., R. N. Thompson, and C. A. Donnelly. 2021. Are epidemic growth rates more informative than reproduction numbers? medRxiv, https://doi.org/10.1101/2021.04.15.21255565.

Park, S. W., B. M. Bolker, S. Funk, C. J. E. Metcalf, J. S. Weitz, B. T. Grenfell, and J. Dushoff. 2021. Roles of generation-interval distributions in shaping relative epidemic strength, speed, and control of new SARS-CoV-2 variants. medRxiv, https://doi.org/10.1101/2021.05.03.21256545.

Pathak, A. K., B. Boag, M. Poss, E. T. Harvill, and I. M. Cattadori. 2011. Seasonal breeding drives the incidence of a chronic bacterial infection in a free-living herbivore population. Epidemiology and Infection 139:1210–1219.

Penczykowski, R. M., E. Walker, S. Soubeyrand, and A.-L. Laine. 2015. Linking winter conditions to regional disease dynamics in a wild plant–pathogen metapopulation. New Phytologist 205:1142–1152.

Poulin, R. 2020. Meta-analysis of seasonal dynamics of parasite infections in aquatic ecosystems. International Journal for Parasitology 50:501–510.

Prati, S., E. H. Henriksen, R. Knudsen, and P.-A. Amundsen. 2020. Seasonal dietary shifts enhance parasite transmission to lake salmonids during ice cover. Ecology and Evolution 10:4031–4043.

Roberts, M., and J. Heesterbeek. 1998. A simple parasite model with complicated dynamics. Journal of Mathematical Biology 37:272–290.

Rohani, P., R. Breban, D. E. Stallknecht, and J. M. Drake. 2009. Environmental transmission of low pathogenicity avian influenza viruses and its implications for pathogen invasion. Proceedings of the National Academy of Sciences of the USA 106:10365–10369.

Scherer, C., V. Radchuk, C. Staubach, S. Müller, N. Blaum, H.-H. Thulke, and S. Kramer-Schadt. 2019. Seasonal host life-history processes fuel disease dynamics at different spatial scales. Journal of Animal Ecology 88:1812–1824.

Suffert, F., V. Ravigné, and I. Sache. 2015. Seasonal changes drive short-term selection for fitness traits in the wheat pathogen *Zymoseptoria tritici*. Applied and Environmental Microbiology 81:6367–6379.

Thieme, H. R. 2003. Mathematics in population biology. Princeton University Press, Princeton, NJ.

Thompson, C., and D. Scott. 1979. Production and persistence of the nuclear polyhedrosis-virus of the Douglas-fir tussock moth, *Orgyia pseudotsugata* (Lepidoptera, Lymantriidae), in the forest ecosystem. Journal of Invertebrate Pathology 33:57–65.

Treanor, J. J., C. Geremia, M. A. Ballou, D. H. Keisler, P. J. White, J. J. Cox, and P. H. Crowley. 2015. Maintenance of brucellosis in Yellowstone bison: linking seasonal food resources, host-pathogen interaction, and life-history trade-offs. Ecology and Evolution 5:3783–3799.

Valencia-Aguilar, A., L. F. Toledo, M. V. Vital, and T. Mott. 2016. Seasonality, environmental factors, and host behavior linked to disease risk in stream-dwelling tadpoles. Herpetologica 72:98–106.

van den Berg, F., C. A. Gilligan, D. J. Bailey, and F. van den Bosch. 2010. Periodicity in host availability does not account for evolutionary branching as observed in many plant pathogens: an application to *Gaeumannomyces graminis* var. *tritici*. Phytopathology 100:1169–1175.

Van Dijk, J. G., B. J. Hoye, J. H. Verhagen, B. A. Nolet, R. A. Fouchier, and M. Klaassen. 2014. Juveniles and migrants as drivers for seasonal epizootics of avian influenza virus. Journal of Animal Ecology 83:266–275.

References Cited Only in the Online Enhancements

Bender, C., and S. Orszag. 1978. Advanced mathematical methods for scientists and engineers. McGraw-Hill, New York.

Associate Editor: Matthew J. Ferrari
Editor: Jennifer A. Lau

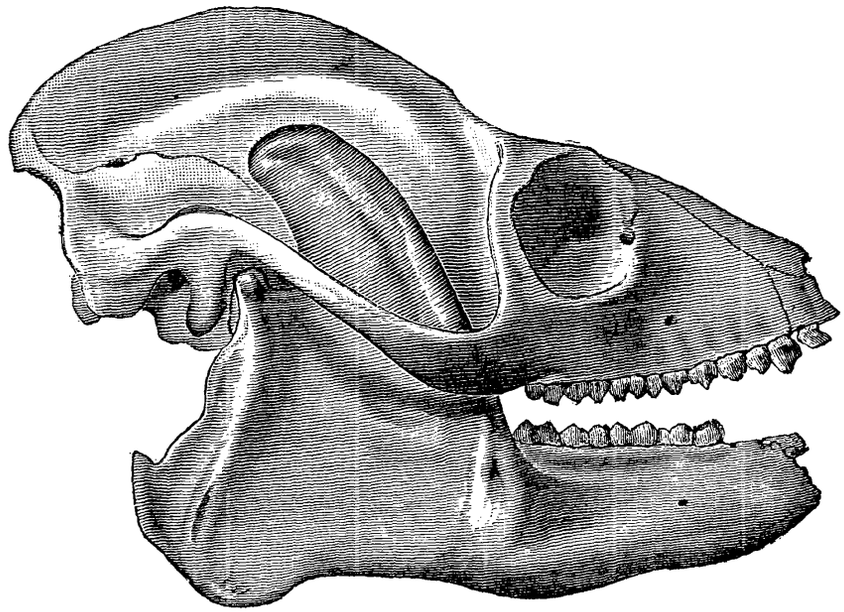

"*Adapis parisiensis* Cuv., . . . from the Phosphorites of Central France. From Filhol." From "The Lemuroidea and the Insectivora of the Eocene Period of North America" by E. D. Cope (*The American Naturalist*, 1885, 19:457–471).